KSÜ Mühendislik Bilimleri Dergisi, 27(3), 2024
Araştırma Makalesi

KSU J Eng Sci, 27(3), 2024
Research Article

Kahramanmaras Sutcu Imam University
Journal of Engineering Sciences

Geliş Tarihi : 26.01.2024
Kabul Tarihi : 17.04.2024

Received Date : 26.01.2024
Accepted Date : 17.04.2024

REMOVAL OF VETERINARY ANTIBIOTICS BY USING LAYERED DOUBLE HYDROXIDE PHOTOCATALYSTS: EFFECTS OF REACTION PARAMETERS AND KINETIC MODELLING

TABAKALI ÇİFT HİDROKSİT FOTOKATALİZÖRLER KULLANARAK VETERİNER ANTİBİYOTİKLERİN GİDERİMİ: REAKSİYON PARAMETRELERİNİN ETKİLERİ VE KİNETİK MODELLEME

Merve BARAÇ[1] (ORCID: 0000-0002-1094-6348)
Burcu PALAS[1] (ORCID: 0000-0002-2815-0057)
Gülin ERSÖZ[1*] (ORCID: 0000-0002-5875-5946)

[1] Ege Üniversitesi, Mühendislik Fakültesi, Kimya Mühendisliği Bölümü, İzmir, Türkiye

*Sorumlu Yazar / Corresponding Author: Gülin ERSÖZ, gulin.ersoz@ege.edu.tr

ABSTRACT

The photocatalytic performances of Ni-Fe-LDH, Co-Fe-LDH, and Cu-Fe-LDH, (LDH: Layered Double Hydroxide) were investigated for the removal of oxytetracycline hydrochloride (OTC-HCl) from water. Layered double hydroxide materials were synthesized by using the co-precipitation method. The photocatalysts were characterized by SEM, XRD, XPS, and BET surface area analyses. The highest pharmaceutical removal efficiency was obtained by using Ni-Fe-LDH photocatalyst. Box-Behnken design was used to examine the influences of reaction parameters on OTC-HCl removal and to determine the optimal reaction conditions. In the parametric study, the interactive influences of photocatalyst loading, solution pH, and the initial oxidant concentration on oxytetracycline hydrochloride removal were investigated. Under visible light irradiation, the optimal conditions were determined to be 1.5 g/L catalyst loading, pH 5, and 1.48 mM H_2O_2 concentration by using Ni-Fe-LDH photocatalyst. OTC-HCl degradation was calculated as 67.1% under the optimal conditions. Hydroxyl radical was determined to be the main effective reactive. Phytotoxicity tests were performed using *Lepidium sativum* seeds. Veterinary antibiotic degradation fit to first order reaction. The Arrhenius constant and activation energy were evaluated as 2.6 min^{-1} and 14.21 kJ/mol, respectively.

Keywords: Layered double hydroxide, tetracycline antibiotics, photocatalytic oxidation, kinetic modelling

ÖZET

Oksitetrasiklin hidroklorik asidin (OTC-HCl) sudan uzaklaştırılması için Ni-Fe-TÇH, Co-Fe-TÇH ve Cu-Fe-TÇH'nin (TÇH: Tabakalı Çift Hidroksit) fotokatalitik performansları araştırılmıştır. Tabakalı çift hidroksit malzemeler kopresipitasyon yöntemi kullanılarak sentezlenmiştir. Fotokatalizörler SEM, XRD, XPS ve BET yüzey alanı analizleri ile karakterize edilmiştir. En yüksek farmasötik giderim değeri, Ni-Fe-TÇH fotokatalizörünün varlığında elde edilmiştir. Reaksiyon parametrelerinin OTC-HCl giderimi üzerindeki etkilerini araştırmak ve optimum reaksiyon koşullarını belirlemek için Box Behnken tasarımı kullanılmıştır. Parametrik çalışmada fotokatalizör dozu, çözelti pH değeri ve başlangıç oksidan derişiminin oksitetrasiklin hidroklorik asit giderimi üzerine interaktif etkileri incelenmiştir. Ni-Fe-TÇH fotokatalizör kullanılarak görünür ışık altında optimum reaksiyon koşulları 1,5 g/L fotokatalizör dozu, 1,48 mM H_2O_2 konsantrasyonu ve pH 5 olarak belirlenmiştir. Optimum koşullar altında OTC-HCl giderimi %67,1 olarak hesaplanmıştır. Radikal tuzaklama deneylerinde hidroksil radikalinin başlıca etkili reaktif tür olduğu tespit edilmiştir. *Lepidium sativum* tohumları kullanılarak fitotoksisite testleri gerçekleştitlmiştir. Kinetik çalışmalarda veteriner antibiyotik bozunmasının birinci dereceden reaksiyon hız

ToCite: BARAÇ, M., PALAS, B., & ERSÖZ, G., (2024). REMOVAL OF VETERINARY ANTIBIOTICS BY USING LAYERED DOUBLE HYDROXIDE PHOTOCATALYSTS: EFFECTS OF REACTION PARAMETERS AND KINETIC MODELLING. *Kahramanmaraş Sütçü İmam Üniversitesi Mühendislik Bilimleri Dergisi*, 27(3), 804-820

modeline uyduğu sonucuna varılmıştır. Aktivasyon enerjisi 14,21 kJ/mol ve ön üstel faktör 2,6 min^{-1} olarak hesaplanmıştır.

Anahtar Kelimeler: Tabakalı çift hidroksit, tetrasiklin antibiyotikler, fotokatalitik oksidasyon, kinetik modelleme

INTRODUCTION

The wastewater contaminated with pharmaceutical drugs constitutes a major international concern for surface waters and drinking waters. Veterinary antibiotics have been used worldwide in large amounts to treat disease and protect animal health. They have been used at large scales in animal farming and pollute water sources through the disposal of metabolized and unmetabolized (expired or unused) antibiotics (Leavey-Roback, Krasner, and Suffet, 2016; Sarmah, Meyer, and Boxall, 2006). In addition, the antibiotics are released into the environment hospital effluents, pharmaceutical industry wastewaters, and runoff from agricultural lands into sewers (Michael et al., 2013; Ngigi, Magu, and Muendo, 2020). In agriculture (poultry, farming of swine, cattle breeding, etc.) use of antibiotics comprises treatment, disease prevention, growth promotion, and control (Done, Venkatesan, and Halden, 2015). Tetracyclines are the most commonly used antibacterial pharmaceuticals followed by sulfonamides. The main tetracycline drugs are chlortetracycline, doxycycline, tetracycline, and oxytetracycline. Tetracyclines are known to be effective against a large number of bacteria from various groups, as well as rickettsia, chlamydia, spirochetes, mycoplasmas, leptospires, and some protozoa (Samanidou, Nikolaidou, and Papadoyannis, 2007). The presence of tetracyclines in the environment may result in serious influences on human health including contribution to antibiotic resistance (Yildirim-Tirgil et al., 2019).

The emerging contaminants in present wastewater discharged from various industries including pharmaceutical, textile, food, etc. have gained attention due to their toxicity and persistence in the environment. The persistence of the organic compounds is assessed by the rates at which they are removed by physical, chemical, and biological processes. Persistent organic pollutants are chemicals whose long-term persistence results in accumulation in the environment and biota due to chronic exposure (Chauhan et al., 2021; Papa and Gramatica, 2008). Antibiotics are regarded as persistent since the rate of entering into the environment is more than the rate of decomposition. Most of the pharmaceuticals including the antibiotics are non-biodegradable and have very stable chemical structures. Antibiotic residues may result in adverse effects such as generation of stable organic by-products, which are difficult to eliminate by the traditional wastewater treatment methods. (Gothwal and Shashidhar, 2015; Rokesh, Sakar, and Do, 2021).

In addition, incomplete mineralization of antibiotics may result in formation of degradation products that are more toxic than the parent compound. Therefore, advanced oxidation methods are good alternatives to treat antibiotic containing wastewater since they are capable of complete mineralization (Adeyemi, Ajiboye, and Onwudiwe, 2021).

Among the many methods applied for pollutant removal, such as adsorption, coagulation-flotation, filtration, and biological treatment, advanced oxidation processes stand out due to the complete degradation of pollutants instead of their transfer from one phase to another. Reactive radicals released in advanced oxidation processes, which have an important role among the environmentally friendly methods applied in wastewater treatment, non-selectively transform a wide range of organic pollutants into H_2O, CO_2, and simple inorganic salts.

Most of the active ingredients in drugs are persistent in the aquatic environment due to their non-biodegradable characteristics. The pharmaceutical residues in water produce hazardous effects in both human bodies and aquatic ecosystems. Endocrine system disruption is one of the important issues arising from the effect of chemicals. Therefore, it is crucial to degrade the drug residues in water before discharging the drug containing wastewater (Gupta et al., 2022).

Most of the traditional wastewater treatment methods are insufficient to decompose the persistent compounds. Advanced oxidation processes are promising technologies to eliminate the persistent pharmaceuticals in wastewater through the formation of hydroxyl radicals (Lin et al., 2017). Among the advanced oxidation processes, photocatalysis and photo Fenton-like oxidation have received attention since these methods are cost-effective and environmentally friendly in comparison to many other wastewater treatment processes. Organic contaminants can be mineralized completely by using photocatalytic oxidation in contrast to nondestructive treatment methods such as coagulation and adsorption. In these processes, various reactive species including $^{\bullet}OH$, $^{\bullet}O_2^-$, and h^+ are formed in the presence of photocatalysts (Bagherzadeh, Kazemeini, and Mahmoodi, 2021). Therefore, the development of

inexpensive and effective photocatalysts for the decomposition of persistent organic pollutants has become a significant research area.

Layered double hydroxide (LDH) materials which are known to be anionic clays and hydrotalcite-like materials have gained attention for the effective elimination of organic pollutants in wastewater. Layered double hydroxides consist of exchangeable interlayer anions, divalent and trivalent metals, and interlayer anions. Due to their large surface area, crystal structure, and molecular stability, layered double hydroxides are among the promising multifunctional materials for applications in wastewater treatment. By using layered double hydroxides containing copper and iron ions, peroxide activation can be achieved with negligible metal leaching. Due to their anion exchange capacity, and the ability to capture inorganic and organic anions, layered double hydroxides have a great potential to be used in catalytic processes, ion exchange, adsorption, photochemical and electrochemical applications (F. Li and Duan, 2005; Yan et al., 2017).

According to the study reported in the literature, the layered double hydroxides showed a promising performance for the removal of antibiotics from water. For instance, Ao et al. (2019) studied middle pressure UV/peroxymonosulfate (MPUV/PMS) oxidation in the presence of sulfate radical to remove tetracycline in water. Optimal removal was achieved at an initial tetracycline dosage of 11.25 μm at pH=3.7, a PMS dose of 0.2μm, and a 250 $mJcm^{-2}$ UV light irradiation. As a result, 82% of tetracycline was degraded by the MPUV/PMS system (Ao et al., 2019). Chen et al. (2019) investigated the photocatalytic performance of Ag_2O/Ag decorated layered double hydroxide catalyst. LDH-Ag_2O/Ag was prepared by depositing Ag_2O on LDH surface and converted into silver nanoparticles after heat treatment. The optimal catalytic efficiency of LDH-Ag_{10} catalysts (0.0184 min^{-1}) was nearly 46 times higher than that of bare layered double hydroxide (0.0004 min^{-1}). Radical quenching experiments showed that •OH is the dominant reactive oxygen species whereas h^+ and $•O_2^-$ have also affected the tetracycline oxidation (C. R. Chen et al., 2019). Fan et al. (2012) studied anion exchange precipitation process to prepare bifunctional Ag/AgBr/Co–Ni–NO_3 LDH nanocomposites. It was observed that Ag/AgBr nanoparticles were widely spread on Co–Ni–NO_3LDH layers. Nanocomposites have been used to absorb and photocatalytically decompose organic pollutants from water. For the removal of dyes and phenol, the catalytic activities of nanocomposites were found to be higher than Co–Ni–Br LDH and Ag/AgBr. This method may be preferred for the preparation of other LDH/silver salt compositions. It was concluded that these kinds of nanostructures have extensive applications in treatment due to their high absorption capacity and high photocatalytic activity (Fan et al., 2013).

Panplado et al. (2019) studied on degradation of tetracycline antibiotics from wastewater. In situ-adsorption method includes formation of mixed metal hydroxide materials which act as an adsorbent for tetracycline removal from aqueous solutions, by using the components of layered double hydroxide materials under alkaline conditions. 100% removal of tetracycline was achieved under optimized conditions. Recovery of tetracycline was tested in the presence of various anions. Due to the high charge density, 98% recovery was obtained by using phosphate (Panplado et al., 2019). Zhu et al. (2021) analyzed the photocatalytic removal performance of Cu-Fe/LDH@$BiOI_{1.5}$ photocatalyst designed with a simple hydrothermal synthesis method. The tests of photocatalytic oxidation of tetracycline indicated that the highest removal reached 73% in 75 minutes in the presence of 1:10 Cu-Fe/LDH@$BiOI_{1.5}$ catalyst. The dominant reactive oxygen species were determined to be $O_2^{•-}$ and h^+ in radical trapping experiments (Zhu et al., 2021).

When the studies in the literature on the oxidation of industrial pollutants in the presence of layered double hydroxide catalysts are evaluated, it is concluded that layered double hydroxide catalysts are effective in antibiotic removal. Though the catalytic activities of several types of layered double hydroxides were tested in literature studies, the comparison of the photocatalytic performances of copper, cobalt, and nickel containing layered double hydroxides, optimization of the reaction conditions by response surface methods and investigation of the reaction kinetics and toxicity assessment under optimized conditions constitute the innovative approaches of this study.

MATERIAL AND METHOD

Chemicals

$Fe(NO_3)_3·9H_2O$ (Merck, 99–102%), $Cu(NO_3)_2·3H_2O$ (Tekkim Kimya), $Co(NO_3)_2.6H_2O$ (Carlo Erba), $Ni(NO_3)_2·6H_2O$ (Merck, 99–102), and sodium hydroxide (Merck, ≥99%) were used to prepare layered double hydroxide catalysts. Hydrogen peroxide (H_2O_2, Merck, 35%) and oxytetracycline hydrochloride ($C_{22}H_{24}N_2O_9·HCl$,

Doğa İlaç) were used as the oxidant and the target veterinary antibiotic, respectively, in the photocatalytic experiments.

Catalyst Preparation

Layered double hydroxides were prepared according to the co-precipitation method adopted from the literature (Khataee et al., 2019; Mandal, Mayadevi, and Kulkarni, 2009; Mikami et al., 2016; Z. Shi, et al., 2020). The trivalent metal nitrate (iron nitrate nonahydrate) and the divalent metal nitrate (nitrate salt of copper, cobalt, or nickel) were dissolved in pure water by setting the molar ratio of M^{3+}/M^{2+} to 1/3. 2 N NaOH solution was added into the solution dropwise until the pH of the solution reaches to 10. The resulting mixture was stirred vigorously. The resulting precipitates were filtered, aged at ambient conditions, and dried in an oven at 80 °C for 8 h to obtain the layered double hydroxide photocatalysts.

Catalyst Characterization

The surface texture of the layered double hydroxides was analyzed by a Thermo Scientific Apreo S Scanning Electron Microscopy and the chemical states of elements present on a sample surface were examined via a Thermo Scientific K-Alpha X-Ray Photoelectron Spectrometer in Ege University Application and Research Center for Testing and Analysis. The phases of the layered double hydroxides were analyzed via a Philips X'Pert Pro X-Ray Diffractometer and the surface area measurements were performed by using Mikromeritics Gemini V analyzer in Izmir Institute of Technology Materials Research Center.

Experimental System and Procedure

The photocatalytic oxidation of oxytetracycline hydrochloride (OTC-HCl) was performed in a beaker by using a temperature-controlled hot plate. An 80-Watt halogen lamp was used as a visible light source. In a typical run, 200 mL of 50 ppm OTC-HCl solutions are prepared and the pH of the pharmaceutical solutions is adjusted to the desired values by the addition of HCl or NaOH solutions. After the addition of catalyst, the experiments are carried out in darkness for 30 minutes to reach equilibrium. Subsequently, the required amount of hydrogen peroxide is added and the visible lamp is turned on. The photocatalysis lasted for 60 minutes. Samples are taken periodically to analyze the OTC-HCl degradation.

Experimental Plan

The photocatalytic performances of Ni-Fe-LDH, Co-Fe-LDH, and Cu-Fe-LDH were tested at pH 4 and 1 g/L catalyst loading in the presence and the absence of hydrogen peroxide comparatively. After the most effective layered double hydroxide was selected, the interactive influences of catalyst dose, pH, and H_2O_2 dosage on OTC-HCl degradation were studied in the presence of the chosen catalyst. The experimental plan was determined based on Box–Behnken design. The factors and their levels used in the parametric study are listed in Table 1.

Table 1. Boundaries of the Experimental Design and Coded and Actual Values of the Reaction Parameters

Variable	Symbol	Ranges of levels		
		-1	0	1
Initial pH	X_1	4	7	10
Catalyst Loading, g/L	X_2	0.5	1.5	2
$[H_2O_2]_o$, mM	X_3	0	1	2

The generation of hydroxyl radicals in the photo Fenton-like oxidation process by using layered double hydroxides was analyzed by radical trapping experiments. Isopropanol and methanol were used as hydroxyl radical scavengers (C. Li et al., 2018; S. Li and Hu, 2016). Under the optimal conditions, kinetic studies were conducted at 25°C, 35°C, and 45°C to evaluate the activation energy and to obtain the reaction rate equation expressing the photocatalysis of OTC-HCl by using the most effective layered double hydroxide.

Analysis

Adsorption and photocatalytic degradation of OTC-HCl was determined by spectrophotometric analysis according to the literature studies (F. Chen et al., 2016; Kang, Xu, and Shi, 2019; B. Liu et al., 2019; Luo et al., 2015; W. Shi et al., 2020). The decrease in OTC-HCl concentration during the photocatalytic oxidation was determined by measuring the absorbance values in a UV-VIS Spectrophotometer. The absorbance was measured at 275 nm since the rings containing N-groups which are associated with the absorbance at 275 nm are harder to open when compared

to the other rings in the OTC-HCl molecule (Soltani, Tayyebi, & Lee, 2019). OTC-HCl degradation was evaluated according to Equation 1:

$$\text{OTC-HCl Degradation, \%} = \frac{[C]_o - [C]_t}{[C]_t} \times 100 \quad (1)$$

C_o: The initial OTC-HCl concentration, ppm
C_t : OTC-HCl concentration at time t, ppm

Toxicity Tests

Toxicity tests were performed to determine whether toxic oxidation products are formed during the photocatalytic oxidation (Hoekstra, Bosker, and Lantinga, 2002; Palas, Ersöz, and Atalay, 2019). The toxicity based on growth inhibition was evaluated by measuring the root length of the seeds grown in treated and untreated OTC-HCl solutions and in water. 5 mL treated and untreated OTC-HCl solutions and water were added into separate petri dishes containing *Lepidium sativum* seeds. The seeds were incubated for 3 days in darkness. After 3 days, lengths of the roots growing in different mediums were measured and the inhibition of root growth was calculated based on Eq. 2:

$$\text{Root Growth Inhibition,\%} = \left[\frac{L_C - L_P}{L_C}\right] \times 100 \quad (2)$$

L_C: Mean length of roots of *L. sativum* growing in water (control medium), cm
L_P: Mean length of roots of *L. sativum* roots growing in treated or untreated OTC-HCl solutions, cm

EXPERIMENTAL RESULTS AND DISCUSSIONS

Characterization of Catalysts

Investigation of Surface Morphology

The SEM images of layered double hydroxides are shown in Figure 1. Scanning electron microscope images are recorded at 50000x and 100000x magnifications. As seen in Figure 1, Cu-Fe-LDH catalyst structure is almost homogeneous, and leaf like structures are observed on the surface. Co-Fe-LDH micrographs show that plate-like particles are aggregated and piled indicating the formation of layered double structures. Ni-Fe LDH catalyst samples present aggregates of poorly defined shapes. Ni-Fe-LDH consists of thin layers and coacervates which is the typical product of the co-precipitation method.

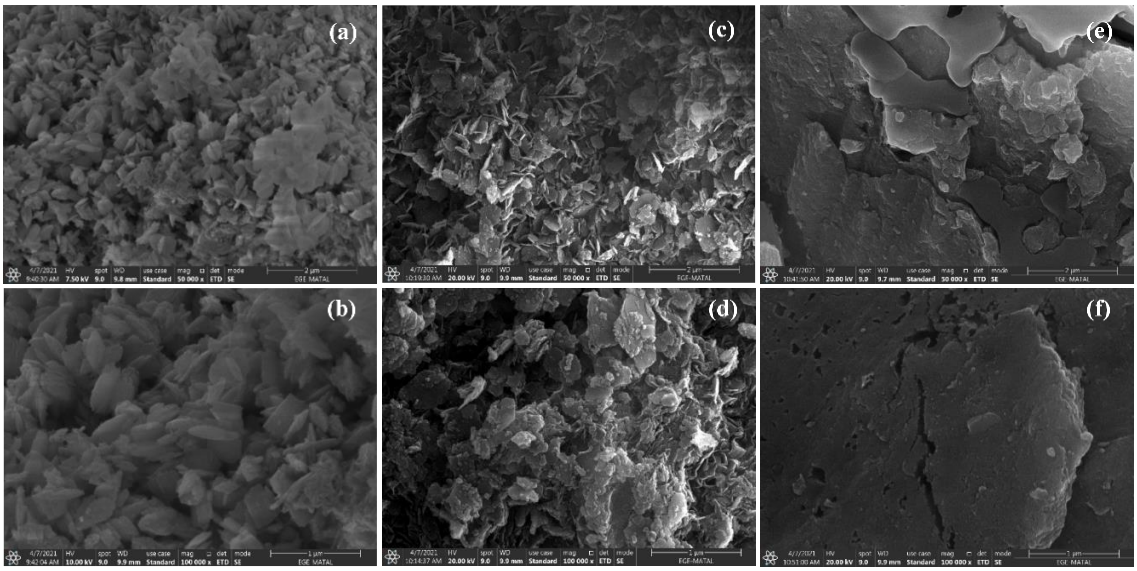

Figure 1. Scanning Electron Micrographs of Cu-Fe-LDH (a,b), Co-Fe-LDH (c,d), and Ni-Fe-LDH (e,f) Recorded at 50000 and 100000 Times Magnifications

XRD Analysis

X-ray diffraction analyses were carried out to determine the composition and structural parameters of layered double hydroxide photocatalysts. XRD pattern of Ni-Fe-LDH Cu-Fe-LDH, and Co-Fe-LDH are presented in Figure 2.

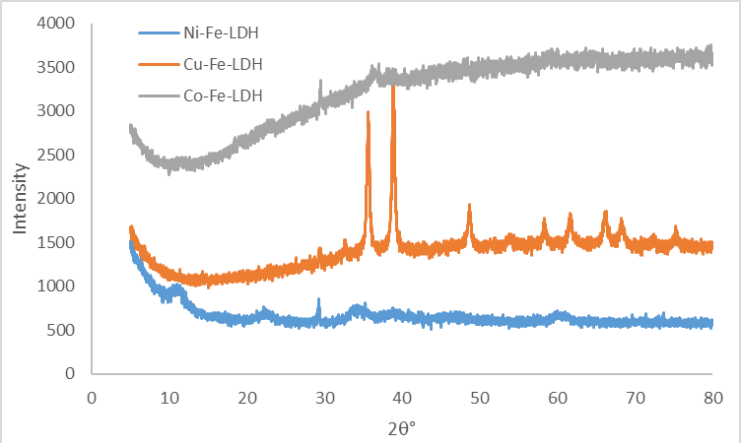

Figure 2. XRD Pattern of LDH Photocatalysts

The XRD pattern of Ni-Fe LDH catalyst shows the characteristic peaks of hydrotalcite-like compounds. The sharp and high-intensity peaks indicate the formation of crystalline structures instead of amorphous structures. Well-defined peaks at 11.6°, 35.5°, and 62.9° are assigned to the (003), (009), and (113) planes of the Ni–Fe LDH, respectively, which confirms that the layered double hydroxide crystals are formed (J. Chen et al., 2018; Ren et al., 2019; Sirisomboonchai et al., 2019). The peaks at 29.3° and 50.8° are associated with the impurities of $Ni_{0.6}Fe_{2.4}O_4$ phase (Anantharaj et al., 2017) and Ni–Fe alloys (Rosmini et al., 2022).

The diffraction peaks at 27.1°, 29.5, 36.1°, and 55.2° are indexed into (006), (105), (015), and (110) planes of Co-Fe-LDH (Arif et al., 2019). Cu-Fe LDH displayed several sharp diffraction peaks at 35.9°, 38.9°, 48.5°, 58.0°, 61.8°, 63.2°, 66°, 68.2°, and 75.2°. The XRD pattern showed that Cu-Fe-LDH was well crystallized with a typical layered structure. In the literature, similar XRD patterns are reported for Cu-Fe LDH (L. Liu et al., 2019).

Surface Analysis

The results of BET surface area measurements performed for Cu-Fe LDH, Ni-Fe LDH, and Co-Fe photocatalysts are presented in Table 2, and the N_2 adsorption isotherms are shown in Figure 3.

Table 2. Surface Area, Pore Volume, and Size Results for LDH Photocatalysts

	Cu-Fe LDH	Ni-Fe LDH	Co-Fe LDH
BET Surface Area, m^2/g	35.65	2.55	22.63
Pore Volume, cm^3/g	0.134	0.125	0.164
Pore Size, Å	150.62	336.19	289.1

The surface areas of the layered double hydroxides prepared in this study and the literature studies are similar. For instance, Utami et al. (2022) reported that the surface area of NiAl LDH is 3.288 m^2/g (Utami, Ahmad, Zahara, Lesbani, and Mohadi, 2022). Wei et al. (2022) revealed that the surface areas of Mg-Al-Cl LDHs and Ca-Al-CO_3-LDHs were 8.4 and 7.6 m^2/g, respectively (Wei, Li, Ye, Rietveld, and van Halem, 2022). N_2 adsorption and desorption isotherms of Ni-Fe-LDH are presented in Figure 3.

The adsorption and desorption isotherms of LDH photocatalysts corresponded to Type III isotherms indicating a multilayer structure according to the IUPAC classification. Type III indicates weak interactions of adsorbent and adsorbate on macroporous adsorbents (Rouquerol et al., 2014). Type-III isotherm is convex with respect to the relative pressure axis throughout the entire range. For each catalyst, the P/P_o value difference between adsorption and desorption was found to be <0, which tells microporous volume is relatively less. Based on the IUPAC classification, the resemblance of H_3 type hysteresis loop reveals the existence of flat particles or slit-shaped pores (L. Liu et al., 2019; Tagliazucca, et al., 2013).

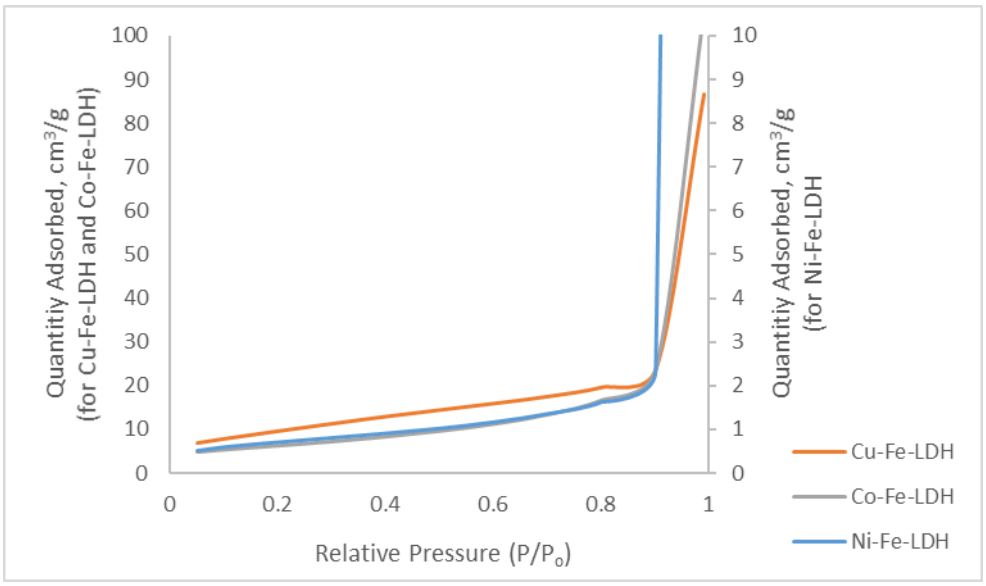

Figure 3. N_2 Adsorption and Desorption Isotherms of Layered Double Hydroxides

XPS Analysis

Valence states of the most effective layered double hydroxide catalyst were determined by XPS analysis and X-ray photoelectron spectra of Ni-Fe-LDH were presented in Figure 4.

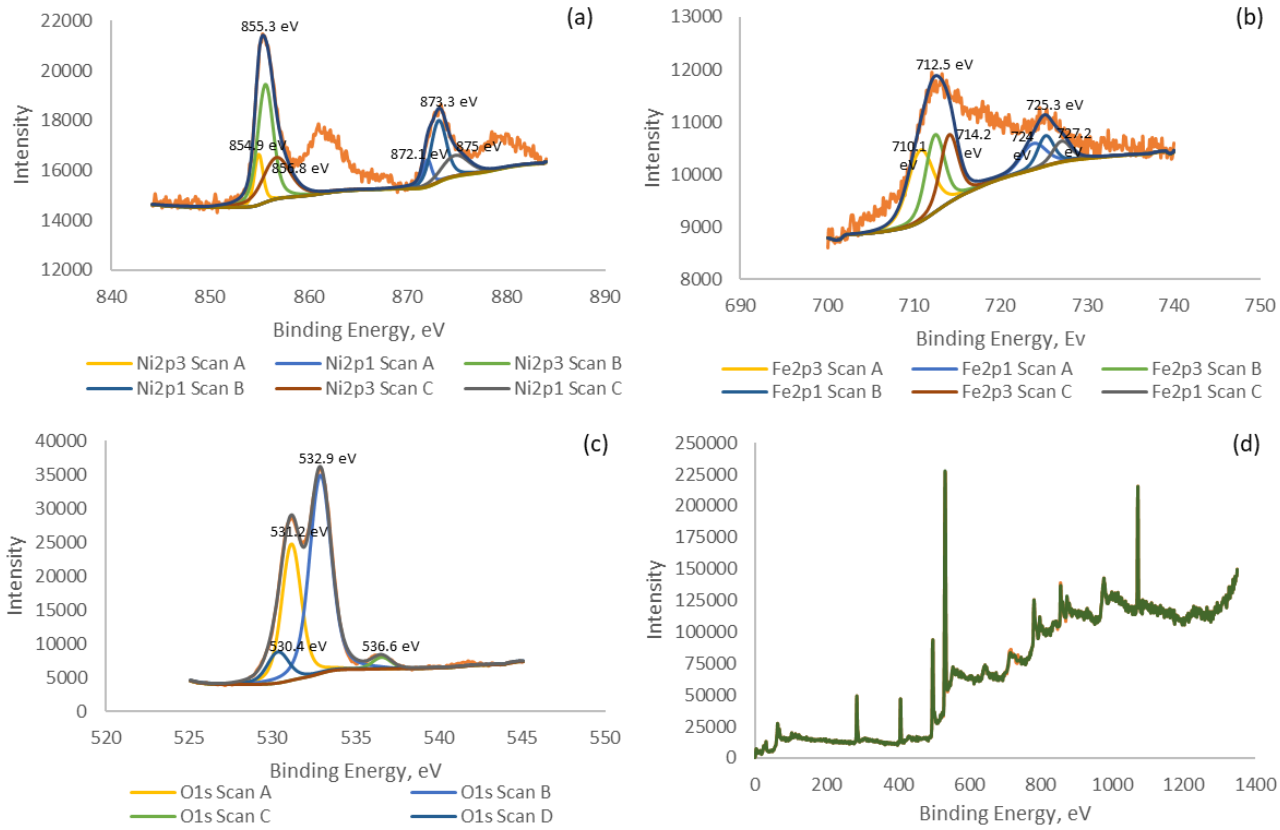

Figure 4. XPS Spectrum of Ni-Fe-LDH Catalyst (a) Ni2p Scan, (b) Fe2p Scan, (c) O1s Scan, and (d) XPS Survey

Figure 4 shows the chemical states of nickel, iron, oxygen, and carbon. In Ni 2p spectrum, the peaks are located at 872.08, 856.78, 855.58, 855.28, and 854.88 eV. The peaks observed at 854.88 eV and 855.28 eV are associated with the presence of Ni-O bond and $Ni(OH)_2$ group, respectively (Mauraya et al., 2022). In Fe 2p spectrum, the peaks are centered at 727.18, 725.28, 723.98, 714.18, 712.48, and 710.88 eV. The peak appeared at 710.88 eV indicating the presence of Fe_2O_3. The peak located at 723.98 eV confirms +3 oxidation state of iron. The peaks are centered at

541.98, 537.18, 536.58, 532.88, 531.18, 530.38 eV. In O1s spectra of Ni-Fe-LDH catalyst, the peaks around 530.38 and 531.18 corresponded to metal-oxygen bond and oxygen defects in the layered double hydroxide, respectively. The peak around 532.88 is attributed to the adsorbed oxygen resulting from hydroxyl groups including adsorbed water (X. Feng et al., 2021; C. Song et al., 2021).

Catalyst Screening

Antibiotic removal performances of Cu-Fe-LDH, Co-Fe-LDH, and Ni-Fe-LDH layered double hydroxides were studied at pH 4 and 1 g/L of catalyst dose under visible light irradiation. The experimental study was carried out in darkness and without oxidant during the first 30 minutes to reach the adsorption equilibrium. After 30 min, photocatalytic oxidation was maintained for 1 hour under visible light with or without using H_2O_2 as an oxidant. In case of using oxidant, H_2O_2 dosage was fixed at 1 mM. The experimental results obtained from the catalyst screening study are presented in Figure 5.

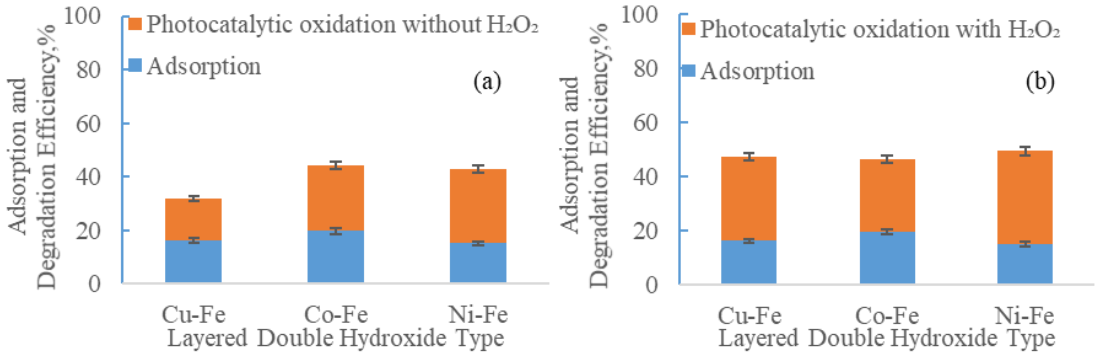

Figure 5. Photocatalytic Activities of Various Layered Double Hydroxides in the Absence (a) and in the Presence of Oxidant (b) (Reaction conditions: pH 4, 1 g/L of catalyst loading)

According to the literature survey, a negligible degradation was observed for the photolysis of tetracycline indicating that was stable in the absence of photocatalyst (B. Liu et al., 2019; Reyes et al., 2006; Wu et al., 2020). The experimental results show that the adsorption performances of the layered double hydroxides varied between 15.1% and 19.7%. The highest photocatalytic degradation efficiency was obtained by using a Ni-containing catalyst. The photocatalytic degradation efficiencies of OTC-HCl were evaluated as 15.4%, 24%, and 27.7% by using Cu-Fe-LDH, Co-Fe-LDH, and Ni-Fe-LDH, respectively, whereas these efficiencies increased to 31.1%, 26.9%, and 34.4% in the presence of H_2O_2. The highest cumulative antibiotic removal including the adsorption and photocatalytic oxidation was calculated as 49.5% in the presence of Ni-Fe-LDH catalyst.

Interactive Influences of Reaction Parameters

Ni-Fe LDH, which provides the most effective removal, was used in the parametric study. As in the catalyst screening, the experiments were carried out in two sections including the adsorption performed in darkness and the subsequent photocatalysis under visible light irradiation. The parametric study plan was formed based on the Box-Behnken design using the Minitab17 program. The response surface methodology was applied to determine the interactive influences of process variables on antibiotic removal with a confidence level of 95%. The upper and lower limits of the oxidation parameters were 4-10 for pH, 0.5-1.5 g/L for catalyst loading, and 0-2 mM for H_2O_2 dosage. The response surface plots showing the interactive influences of catalyst loading (CL), initial pH, and the initial H_2O_2 dosage (HPC) are presented in Figure 6.

In photo Fenton oxidation processes, the organic pollutants were decomposed and reacted with the hydroxyl radicals mainly generated in the following reactions:

$$Fe(OH)^{2+} + h\nu \rightarrow Fe^{2+} + HO^{\bullet}$$
$$Fe^{2+} + H_2O_2 \rightarrow Fe(OH)^{2+} + HO^{\bullet}$$

The reactions of hydroxyl radicals with organic compounds containing C-H or C=C bonds generally proceed with rate constants approaching the diffusion-controlled limit. For this reason, oxidation rates are generally limited by the

rates of hydroxyl radical formation and competition by other hydroxyl radical scavengers in reaction medium rather than by reactivity with the oxidant (Haag and David Yao, 1992).

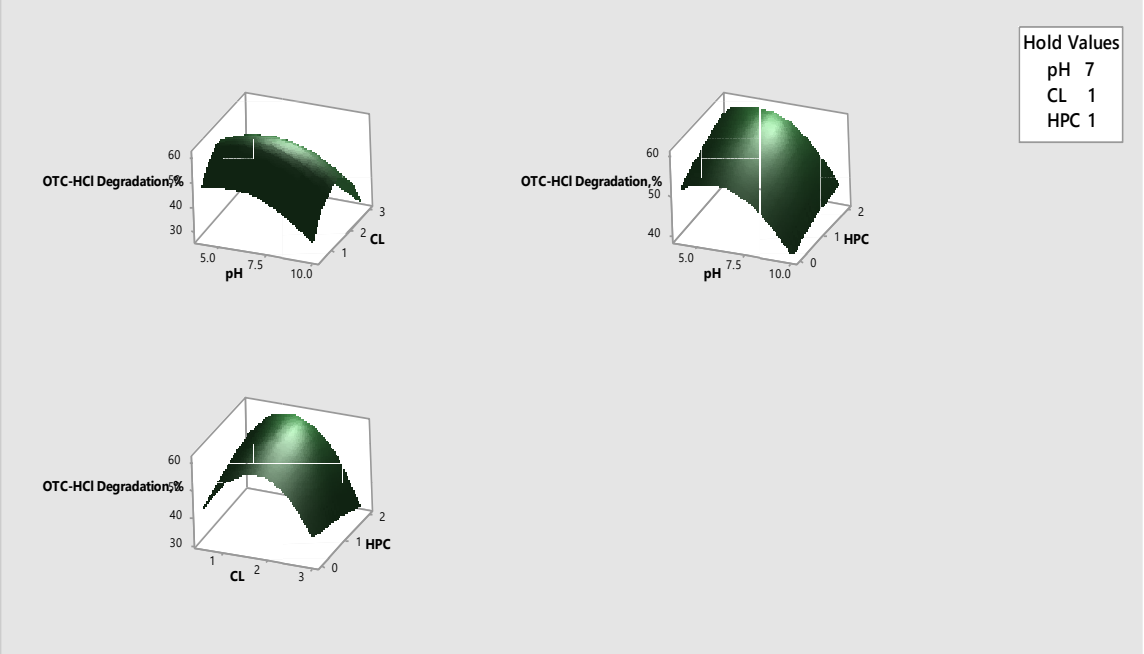

Figure 6. Surface Plots Showing the Interactive Influences of pH and CL (a), pH and HPC (b), and CL and HPC (c) on OTC-HCl Degradation

Catalyst loading is one of the important parameters affecting the hydroxyl radical formation and performance of Fenton oxidation-based processes. In the presence of Ni-Fe-LDH reactive oxygen species are formed in the reactions between the oxidant and both of the ferric and nickel ions. From Figures 6a and 6c, it is concluded that OTC-HCl removal was improved by increasing the catalyst loading up to the optimal value. The enhancement of antibiotic degradation efficiency can be explained by the increase in the number of active sites on the surface of the catalyst at a higher catalyst loading (Q. Feng et al., 2020). However, above the optimal catalyst dose, the removal efficiencies can be explained by $^{\bullet}OH$ scavenging resulting from the excess iron and nickel species. Additionally, light penetration through the reaction medium is reduced at high catalyst loadings and the total number of photons that could reach hydrogen peroxide molecules decreases (Kasiri, Aleboyeh, and Aleboyeh, 2008). Kerchich et al. (2021) reported that the dye removal efficiencies increased up to 0.5 g/L δ-Fe_2O_3/MgAl-LDH photocatalyst dose due to the increase in absorption sites on the catalyst surface leading to the formation of hydroxyl radicals. However, above the optimum photocatalyst dosage, the removal efficiencies decreased due to the reduction of the light penetration and the agglomeration of the photocatalyst particles (Kerchich, et al., 2021).

Figures 6a and 6b depicted that increasing the initial pH resulted in decrease in OTC-HCl degradation. Fenton-based processes at acidic conditions. The lower degradation efficiency at high pH values can be attributed to the decomposition of hydrogen peroxide into water and oxygen which reduces the formation of $^{\bullet}OH$ (Arshadi et al., 2016). Moreover, the performance of Fenton-based processes decreases at basic conditions due to the tendency to formation of $HO_2^{\bullet}$ that is less reactive than $^{\bullet}OH$.

Similarly, the improvement of antibiotic degradation in acidic medium by using layered double hydroxide catalysts is reported in literature studies. Sahoo et al. (2019) reported that tetracycline degradation efficiency is maximum at pH 4.5 since in a weak acidic environment, hydrogen ions can easily react with $^{\bullet}O_2^-$ to generate $^{\bullet}OH$ (Sahoo, Patnaik, and Parida, 2019). Song et al. (2022) stated that the photocatalytic performance of Ce/TiO_2@LDH decreases with the increase of pH value due to the hydroxide anions coming from high pH conditions reacted with hydroxyl radicals, resulting in the deactivation of hydroxyl radicals (Z. Song, Gao, Liao, Zhang, and Wang, 2022).

The increase in oxidant dosage favored antibiotic degradation. Studies in the literature are also consistent with the fact that the use of hydrogen peroxide increases antibiotic removal up to the optimal dosage. For instance, Gholami et al. (2020) revealed that the addition of hydrogen peroxide favored the photocatalytic degradation of gemifloxacin

antibiotic using Zn-Co-LDH@biochar photocatalyst (Gholami, Khataee, Soltani, Dinpazhoh, and Bhatnagar, 2020). However, the excessive use of oxidant also reduces the degradation efficiencies. Yang et al. (2022) revealed that in the presence of FeNi-LDH/Ti_3C_2, the tetracycline degradation efficiency was remarkably decreased at high H_2O_2 concertation since excessive H_2O_2 quench the hydroxyl radicals to produce hydroperoxyl radicals which further consume the hydroxyl radicals (Yang et al., 2022).

The variation in H_2O_2 dosage was less effective than pH. It is recommended to operate near the upper boundary of oxidant dosage in an acidic medium to reach the highest OTC-HCl degradation.

By the synergetic effect of H_2O_2 and metal ions (M), hydroxyl radicals are formed in the following reaction:

$$M^{n+} + H_2O_2 \rightarrow M^{n+1} + HO^{\bullet} + OH^{-}$$

To examine the interactive influences of catalyst and H_2O_2 loadings, the catalyst loading was changed in the range of 0.5 and 1.5 g/L whereas the pH varied between 4 and 10. Figure 5c depicts that catalyst loading was more effective in comparison to hydrogen peroxide dosage since the variation in antibiotic degradation efficiency with respect to catalyst loading was higher than the variation with respect to oxidant dosage.

Response Optimization

The optimal photo Fenton-like oxidation conditions were decided by maximizing the OTC-HCl degradation. Catalyst dose, pH, and the initial H_2O_2 dosage were optimized at 1.5 g/L, 5, and 1.48 mM, respectively, and the degradation efficiency is predicted as 68.7%. A set of experiments were conducted at the optimal conditions to test the accuracy of the model by the comparison of the predicted and the experimental degradation efficiencies. Under the optimal conditions, 67.1% OTC-HCl degradation was achieved. The error was calculated as approximately 2.3%. Since the calculated error is below 10%, the model equation can be accepted as accurate and used to predict the degradation at any reaction condition in the range of the defined upper and lower boundaries of reaction parameters. The decrease in OTC-HCl concentration under the optimal conditions is shown in Figure 7.

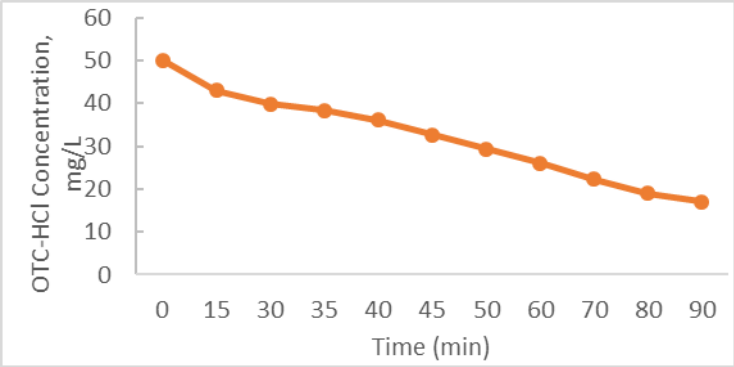

Figure 7. The Decrease in OTC-HCl Concentration under the Optimum Photocatalytic Conditions

Radical Quenching Experiments

To determine whether •OH radicals are generated during the photo Fenton-like reactions, OTC-HCl degradation was calculated both in the presence and absence of hydroxyl radical scavengers. Radical trapping studies were performed at the optimal operating conditions by adding isopropanol or methanol separately. The degradation efficiencies obtained by the addition of radical quenchers are given in Figure 8.

Antibiotic degradation efficiencies decreased by the addition of methanol and isopropanol significantly. OTC-HCl degradation efficiencies were evaluated as 27.4% and 18.5% by using methanol and isopropanol, respectively. The results demonstrated that mainly •OH was involved and played an effective role in OTC-HCl degradation.

Toxicity Tests

In the context of this study, the photocatalytic conditions including the photocatalyst and oxidant dosages and pH were optimized by using response surface methodology and Box-Behnken Design. The toxicity of the photocatalytic oxidation products was analyzed for the optimized reaction conditions which are recommended for practical

applications in further studies. Toxicity tests were performed to assess the toxicity of the intermediates and end products generated during the photocatalytic oxidation of OTC-HCl by using layered double hydroxides.

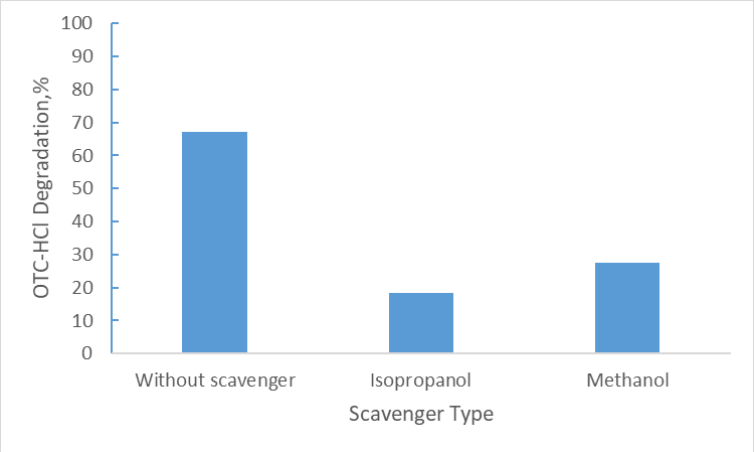

Figure 8. Radical Trapping Experimental Results

The mean root lengths of *L. sativum* roots growing in treated and untreated OTC-HCl solutions were 19.46 and 14.66 mm, respectively, whereas the mean length of the roots growing in water was 37.13 mm. The toxicity of the untreated and treated pharmaceutical solutions in terms of growth inhibition was calculated as 60.51% and 47.59%, respectively. Since the growth inhibition was reduced by 12.92% after the photo Fenton-like oxidation treatment in the presence of Ni-Fe-LDH catalyst, it is determined that this treatment method and Ni-Fe-LDH photocatalyst were effective in decreasing the toxicity of OTC-HCl solutions.

Kinetic Study

Kinetic studies were conducted to derive reaction rate equation expressing photocatalytic degradation of the parent compound, OTC-HCl using layered double hydroxides. The kinetic study on oxytetracycline hydrochloride degradation in the presence of Ni-Fe-LDH was carried out in a temperature range of 25-45°C under the optimal reaction conditions which were determined as pH 5, 1.5 g/L catalyst loading, and 1.48 mM H_2O_2 dosage. The initial OTC-HCl dosage was fixed at 50 mg/L in the kinetic study. For the determination of the most suitable kinetic model for the kinetic data, power rate models, which are the most commonly used reaction kinetic models, were proposed and the most appropriate reaction rate expression was determined by comparing the regression coefficients. The suitability of the 1st and 2nd order reaction rate models given in Equations 3 and 4 were tested by the application of regression analysis.

$$\frac{dC_{OTC\text{-}HCl}}{dt} = -k_1 C_{OTC\text{-}HCl} \quad \text{by integrating:} \quad \ln\frac{[C_{OTC\text{-}HCl_o}]}{[C_{OTC\text{-}HCl}]} = k_1 t \tag{3}$$

$$\frac{dC_{OTC\text{-}HCl}}{dt} = -k_2 C_{OTC\text{-}HCl}^{\,2} \quad \text{by integrating:} \quad \frac{1}{[C_{OTC\text{-}HCl}]} = \frac{1}{[C_{OTC\text{-}HCl}]_o} + k_2 t \tag{4}$$

where $C_{OTC\text{-}HCl}$ [mg/L] is the concentration of OTC-HCl, k_1 [min^{-1}] and k_2 [$L.mg^{-1}min^{-1}$] are the first and second-order reaction rate constants, respectively, and t [min] is the reaction time.

The graphics showing the 1st and the 2nd order reaction rates and corresponding regression coefficients are presented in Figure 9, and the calculated values of the kinetic parameters are tabulated in Table 3.

Table 3. Regression Coefficients and Rate Constants Calculated based on the 1st and 2nd Order Reaction Rate Models

	1st Order Reaction Rate Model		2nd Order Reaction Rate Model	
	k_1 [min^{-1}]	R^2	k_2 [$L.mg^{-1}.min^{-1}$]	R^2
25°C	0.0081	0.93	0.0002	0.88
35°C	0.0105	0.94	0.0003	0.878
45°C	0.0116	0.95	0.0004	0.88

k: Reaction rate constant, R^2: Regression coefficient

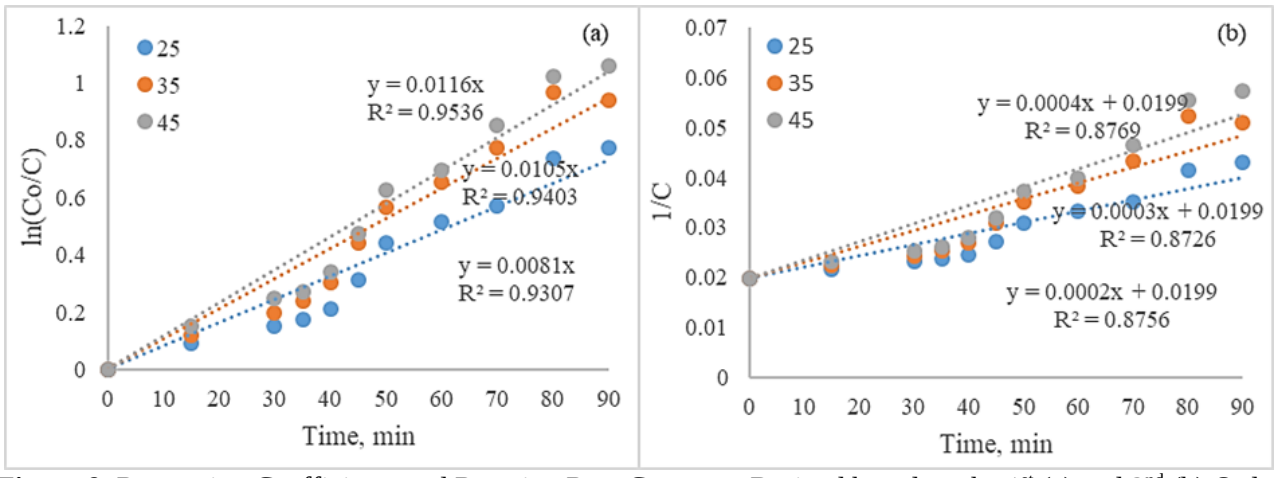

Figure 9. Regression Coefficients and Reaction Rate Constants Derived based on the 1st (a) and 2nd (b) Order Reaction Rate Models

As the reaction temperature rose from 25°C to 45°C, the reaction rate constants increased due to the faster antibiotic degradation. The high R^2 values varying between 0.93 and 0.96 indicated that the 1st order reaction rate model fit well with the antibiotic degradation data. It has been reported in many literature studies that the tetracycline degradation in photo Fenton oxidation processes follows first-order reaction kinetics (Lu et al., 2023; Palanivel et al., 2021; Thi et al., 2022; Yuan et al., 2023).

The Arrhenius plot of photo Fenton-like oxidation of OTC-HCl by using Ni-Fe-LDH (Figure 10) was drawn by using first-order rate constant. The activation energy and Arrhenius constant were determined as 14.21 kJ/mol and 2.58 $L.mg^{-1}min^{-1}$, respectively. This value is slightly higher than the activation of the diffusion controlling reactions, which is usually in the range of 10–13 kJ/mol indicating that the intrinsic chemical reactions on the catalyst surface are more effective than the rate of mass transfer (Zhou et al., 2022).

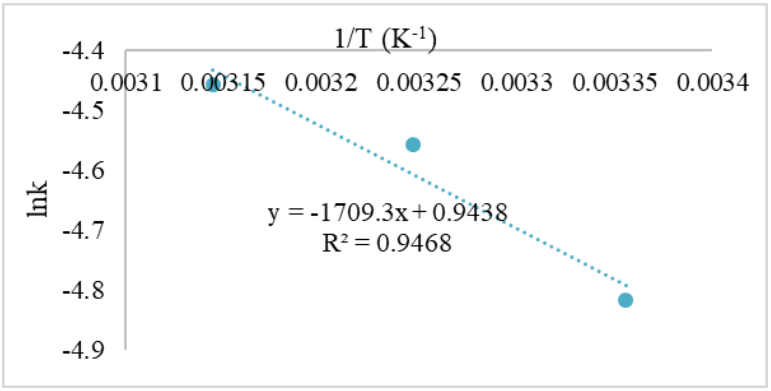

Figure 10. Arrhenius Plot Drawn based on the 1st Order Reaction Rate Model

In literature, the reported values of activation energies calculated for photo-Fenton like oxidation of tetracycline antibiotics are usually similar to or higher than activation energy value determined in this study. For instance, Yuan et al. (2023) reported 39.8 kJ/mol of activation energy for tetracycline hydrochloride removal in the presence of Fe_3S_4/g-C_3N_4 catalyst (Yuan et al., 2023). Thi et al. (2022) evaluated the activation energy as 17.91 kJ/mol for tetracycline removal in the presence of Prussian blue decorated g-C_3N_4 as photo-Fenton catalyst (Thi et al., 2022). Zhou et al. (2022) evaluated the activation energy as 27.88 kJ/mol for tetracycline hydrochloride removal by using Fe_3S_4/MoS_2 catalyst (Zhou et al., 2022). Activation energy calculated in the present study is lower than that in the literature, indicating that the tetracycline degradation by photocatalytic reaction requires a relatively low energy and can be easily achieved.

CONCLUSIONS

The photocatalytic performances of various layered double hydroxides including Ni-Fe-LDH, Co-Fe-LDH, and Cu-Fe-LDH were synthesized, and their visible light-driven catalytic activities were compared for the degradation of the

target veterinary antibiotic. Ni-Fe-LDH exhibited the highest photocatalytic performance in photo Fenton-like oxidation. The interactive influences of catalyst dosage, pH, and H_2O_2 dose on OTC-HCl degradation were analyzed, and the reaction conditions were maximized according to Box-Behnken design. Oxytetracycline hydrochloride degradation was optimized at pH 5, 1.5 g/L of catalyst loading, and 1.48 mM H_2O_2 concentration. At the optimal reaction conditions, 67.1% antibiotic degradation was achieved. Hydroxyl radicals were the main reactive active species responsible for the antibiotic degradation. The photo Fenton oxidation of the antibiotic fits the first-order reaction rate model well. The low activation energy showed that rapid reactions occur by using Ni-Fe-LDH catalyst. The toxicity was reduced by 12.92% during the photocatalytic oxidation.

Investigation of the photocatalytic performances of copper, cobalt, and nickel containing layered double hydroxides for the degradation of veterinary antibiotics, optimization of the reaction conditions by response surface methods, and derivation of kinetic models expressing the OTC-HCl degradation in the presence of layered double hydroxides, and toxicity assessment under optimized conditions constitute the innovative approaches of this experimental study.

The results indicated that the Ni-Fe-LDH is a promising and efficient candidate to be used as a photocatalyst in environmentally friendly applications of veterinary pharmaceutical wastewater treatment. The application of efficient wastewater technologies would contribute to the protection of aquatic life and improvement of environmental health by keeping the water sources clean. The kinetic models expressing the pollutant degradation can provide background for scale-up studies and can encourage practical applications of environmentally friendly advanced oxidation methods in wastewater treatment facilities.

ACKNOWLEDGEMENT

This study was supported by Ege University Scientific Research Project Fund [FYL-2020-22394].

REFERENCES

Adeyemi, J. O., Ajiboye, T., & Onwudiwe, D. C. (2021). Mineralization of Antibiotics in Wastewater Via Photocatalysis. *Water, Air, & Soil Pollution*, *232*(5), 219. https://doi.org/10.1007/s11270-021-05167-3

Anantharaj, S., Karthick, K., Venkatesh, M., Simha, T. V. S. V., Salunke, A. S., Ma, L., … Kundu, S. (2017). Enhancing electrocatalytic total water splitting at few layer Pt-NiFe layered double hydroxide interfaces. *Nano Energy*, *39*(June), 30–43. https://doi.org/10.1016/j.nanoen.2017.06.027

Ao, X., Sun, W., Li, S., Yang, C., Li, C., & Lu, Z. (2019). Degradation of tetracycline by medium pressure UV-activated peroxymonosulfate process: Influencing factors, degradation pathways, and toxicity evaluation. *Chemical Engineering Journal*, *361*, 1053–1062. https://doi.org/10.1016/j.cej.2018.12.133

Arif, M., Yasin, G., Shakeel, M., Mushtaq, M. A., Ye, W., Fang, X., … Yan, D. (2019). Hierarchical CoFe-layered double hydroxide and g-C_3N_4 heterostructures with enhanced bifunctional photo/electrocatalytic activity towards overall water splitting. *Materials Chemistry Frontiers*, *3*(3), 520–531. https://doi.org/10.1039/C8QM00677F

Arshadi, M., Abdolmaleki, M. K., Mousavinia, F., Khalafi-Nezhad, A., Firouzabadi, H., & Gil, A. (2016). Degradation of methyl orange by heterogeneous Fenton-like oxidation on a nano-organometallic compound in the presence of multi-walled carbon nanotubes. *Chemical Engineering Research and Design*, *112*, 113–121. https://doi.org/10.1016/j.cherd.2016.05.028

Bagherzadeh, S. B., Kazemeini, M., & Mahmoodi, N. M. (2021). Preparation of novel and highly active magnetic ternary structures (metal-organic framework/cobalt ferrite/graphene oxide) for effective visible-light-driven photocatalytic and photo-Fenton-like degradation of organic contaminants. *Journal of Colloid and Interface Science*, *602*, 73–94. https://doi.org/10.1016/j.jcis.2021.05.181

Chauhan, R., Dinesh, G. K., Alawa, B., & Chakma, S. (2021). A critical analysis of sono-hybrid advanced oxidation process of ferrioxalate system for degradation of recalcitrant pollutants. *Chemosphere*, *277*, 130324. https://doi.org/10.1016/j.chemosphere.2021.130324

Chen, C. R., Zeng, H. Y., Yi, M. Y., Xiao, G. F., Zhu, R. L., Cao, X. J., … Peng, J. W. (2019). Fabrication of Ag_2O/Ag decorated ZnAl-layered double hydroxide with enhanced visible light photocatalytic activity for tetracycline degradation. *Ecotoxicology and Environmental Safety*, *172*(February), 423–431. https://doi.org/10.1016/j.ecoenv.2019.01.080

Chen, F., Yang, Q., Sun, J., Yao, F., Wang, S., Wang, Y., … Zeng, G. (2016). Enhanced Photocatalytic Degradation of Tetracycline by AgI/$BiVO_4$ Heterojunction under Visible-Light Irradiation: Mineralization Efficiency and Mechanism. *ACS Applied Materials & Interfaces*, *8*(48), 32887–32900. https://doi.org/10.1021/acsami.6b12278

Chen, J., Zheng, F., Zhang, S. J., Fisher, A., Zhou, Y., Wang, Z., … Sun, S. G. (2018). Interfacial Interaction between FeOOH and Ni-Fe LDH to Modulate the Local Electronic Structure for Enhanced OER Electrocatalysis. *ACS Catalysis*, *8*(12), 11342–11351. https://doi.org/10.1021/acscatal.8b03489

Done, H. Y., Venkatesan, A. K., & Halden, R. U. (2015). Does the Recent Growth of Aquaculture Create Antibiotic Resistance Threats Different from those Associated with Land Animal Production in Agriculture? *AAPS Journal*, *17*(3), 513–524. https://doi.org/10.1208/s12248-015-9722-z

Fan, H., Zhu, J., Sun, J., Zhang, S., & Ai, S. (2013). Ag/AgBr/Co-Ni-NO_3 Layered Double Hydroxide Nanocomposites with Highly Adsorptive and Photocatalytic Properties. *Chemistry - A European Journal*, *19*(7), 2523–2530. https://doi.org/10.1002/chem.201203408

Feng, Q., Zhou, J., Luo, W., Ding, L., & Cai, W. (2020). Photo-Fenton removal of tetracycline hydrochloride using $LaFeO_3$ as a persulfate activator under visible light. *Ecotoxicology and Environmental Safety*, *198*(April), 110661. https://doi.org/10.1016/j.ecoenv.2020.110661

Feng, X., Shi, Y., Shi, J., Hao, L., & Hu, Z. (2021). Superhydrophilic 3D peony flower-like Mo-doped Ni_2S_3@NiFe LDH heterostructure electrocatalyst for accelerating water splitting. *International Journal of Hydrogen Energy*, *46*(7), 5169–5180. https://doi.org/10.1016/j.ijhydene.2020.11.018

Gholami, P., Khataee, A., Soltani, R. D. C., Dinpazhoh, L., & Bhatnagar, A. (2020). Photocatalytic degradation of gemifloxacin antibiotic using Zn-Co-LDH@biochar nanocomposite. *Journal of Hazardous Materials*, *382*, 121070. https://doi.org/10.1016/j.jhazmat.2019.121070

Gothwal, R., & Shashidhar, T. (2015). Antibiotic Pollution in the Environment: A Review. *CLEAN – Soil, Air, Water*, *43*(4), 479–489. https://doi.org/10.1002/clen.201300989

Gupta, A. D., Singh, H., Varjani, S., Awasthi, M. K., Giri, B. S., & Pandey, A. (2022). A critical review on biochar-based catalysts for the abatement of toxic pollutants from water via advanced oxidation processes (AOPs). *Science of the Total Environment*, *849*(June), 157831. https://doi.org/10.1016/j.scitotenv.2022.157831

Haag, W. R., & David Yao, C. C. (1992). Rate Constants for Reaction of Hydroxyl Radicals with Several Drinking Water Contaminants. *Environmental Science and Technology*, *26*(5), 1005–1013. https://doi.org/10.1021/es00029a021

Hoekstra, N. J., Bosker, T., & Lantinga, E. A. (2002). Effects of cattle dung from farms with different feeding strategies on germination and initial root growth of cress (Lepidium sativum L.). *Agriculture, Ecosystems and Environment*, *93*(1–3), 189–196. https://doi.org/10.1016/S0167-8809(01)00348-6

Kang, N., Xu, D., & Shi, W. (2019). Synthesis plasmonic Bi/$BiVO_4$ photocatalysts with enhanced photocatalytic activity for degradation of tetracycline (TC). *Chinese Journal of Chemical Engineering*, *27*(12), 3053–3059. https://doi.org/10.1016/j.cjche.2019.05.008

Kasiri, M. B., Aleboyeh, H., & Aleboyeh, A. (2008). Degradation of Acid Blue 74 using Fe-ZSM5 zeolite as a heterogeneous photo-Fenton catalyst. *Applied Catalysis B: Environmental*, *84*(1–2), 9–15. https://doi.org/10.1016/j.apcatb.2008.02.024

Kerchich, S., Boudjemaa, A., Chebout, R., Bachari, K., & Mameri, N. (2021). High performance of δ-Fe_2O_3 novel photo-catalyst supported on LDH structure. *Journal of Photochemistry and Photobiology A: Chemistry*, *406*, 113001. https://doi.org/10.1016/j.jphotochem.2020.113001

Khataee, A., Sadeghi Rad, T., Nikzat, S., Hassani, A., Aslan, M. H., Kobya, M., & Demirbaş, E. (2019). Fabrication of NiFe layered double hydroxide/reduced graphene oxide (NiFe-LDH/rGO) nanocomposite with enhanced sonophotocatalytic activity for the degradation of moxifloxacin. *Chemical Engineering Journal*, *375*(June), 122102. https://doi.org/10.1016/j.cej.2019.122102

Leavey-Roback, S. L., Krasner, S. W., & Suffet, I. M. H. (2016). Veterinary antibiotics used in animal agriculture as NDMA precursors. *Chemosphere*, *164*, 330–338. https://doi.org/10.1016/j.chemosphere.2016.08.070

Li, C., Sun, Z., Zhang, W., Yu, C., & Zheng, S. (2018). Highly efficient g-C_3N_4/TiO_2/kaolinite composite with novel

three-dimensional structure and enhanced visible light responding ability towards ciprofloxacin and S. aureus. *Applied Catalysis B: Environmental*, *220*, 272–282. https://doi.org/10.1016/j.apcatb.2017.08.044

Li, F., & Duan, X. (2005). Applications of Layered Double Hydroxides. In *Layered Double Hydroxides* (pp. 193–223). Berlin/Heidelberg: Springer-Verlag. https://doi.org/10.1007/430_007

Li, S., & Hu, J. (2016). Photolytic and photocatalytic degradation of tetracycline: Effect of humic acid on degradation kinetics and mechanisms. *Journal of Hazardous Materials*, *318*(June), 134–144. https://doi.org/10.1016/j.jhazmat.2016.05.100

Lin, L., Wang, H., Jiang, W., Mkaouar, A. R., & Xu, P. (2017). Comparison study on photocatalytic oxidation of pharmaceuticals by TiO_2-Fe and TiO_2-reduced graphene oxide nanocomposites immobilized on optical fibers. *Journal of Hazardous Materials*, *333*, 162–168. https://doi.org/10.1016/j.jhazmat.2017.02.044

Liu, B., Wu, Y., Zhang, J., Han, X., & Shi, H. (2019). Visible-light-driven g-C_3N_4/Cu_2O heterostructures with efficient photocatalytic activities for tetracycline degradation and microbial inactivation. *Journal of Photochemistry and Photobiology A: Chemistry*, *378*(April), 1–8. https://doi.org/10.1016/j.jphotochem.2019.04.007

Liu, L., Li, S., An, Y., Sun, X., Wu, H., Li, J., … Li, H. (2019). Hybridization of Nanodiamond and CuFe-LDH as Heterogeneous Photoactivator for Visible-Light Driven Photo-Fenton Reaction: Photocatalytic Activity and Mechanism. *Catalysts*, *9*(2), 118. https://doi.org/10.3390/catal9020118

Lu, C., Wang, J., Cao, D., Guo, F., Hao, X., Li, D., & Shi, W. (2023). Synthesis of magnetically recyclable g-C_3N_4/$NiFe_2O_4$ S-scheme heterojunction photocatalyst with promoted visible-light-response photo-Fenton degradation of tetracycline. *Materials Research Bulletin*, *158*, 112064. https://doi.org/10.1016/j.materresbull.2022.112064

Luo, B., Xu, D., Li, D., Wu, G., Wu, M., Shi, W., & Chen, M. (2015). Fabrication of a Ag/Bi_3TaO_7 Plasmonic Photocatalyst with Enhanced Photocatalytic Activity for Degradation of Tetracycline. *ACS Applied Materials & Interfaces*, *7*(31), 17061–17069. https://doi.org/10.1021/acsami.5b03535

Mandal, S., Mayadevi, S., & Kulkarni, B. D. (2009). Adsorption of aqueous selenite [Se(IV)] species on synthetic layered double Hydroxide Materials. *Industrial and Engineering Chemistry Research*, *48*(17), 7893–7898. https://doi.org/10.1021/ie900136s

Mauraya, A. K., Mahana, D., Jhaa, G., Pradhan, B. K., Roopa, Tomer, S., … Muthusamy, S. K. (2022). Heterostructure nanoarchitectonics with ZnO/SnO_2 for ultrafast and selective detection of CO gas at low ppm levels. *Ceramics International*, *48*(24), 36556–36569. https://doi.org/10.1016/j.ceramint.2022.08.215

Michael, I., Rizzo, L., McArdell, C. S., Manaia, C. M., Merlin, C., Schwartz, T., … Fatta-Kassinos, D. (2013). Urban wastewater treatment plants as hotspots for the release of antibiotics in the environment: A review. *Water Research*, *47*(3), 957–995. https://doi.org/10.1016/j.watres.2012.11.027

Mikami, G., Grosu, F., Kawamura, S., Yoshida, Y., Carja, G., & Izumi, Y. (2016). Harnessing self-supported Au nanoparticles on layered double hydroxides comprising Zn and Al for enhanced phenol decomposition under solar light. *Applied Catalysis B: Environmental*, *199*, 260–271. https://doi.org/10.1016/j.apcatb.2016.06.031

Ngigi, A. N., Magu, M. M., & Muendo, B. M. (2020). Occurrence of antibiotics residues in hospital wastewater, wastewater treatment plant, and in surface water in Nairobi County, Kenya. *Environmental Monitoring and Assessment*, *192*(1), 18. https://doi.org/10.1007/s10661-019-7952-8

Palanivel, B., Shkir, M., Alshahrani, T., & Mani, A. (2021). Novel $NiFe_2O_4$ deposited S-doped g-C_3N_4 nanorod: Visible-light-driven heterojunction for photo-Fenton like tetracycline degradation. *Diamond and Related Materials*, *112*, 108148. https://doi.org/10.1016/j.diamond.2020.108148

Palas, B., Ersöz, G., & Atalay, S. (2019). Bioinspired metal oxide particles as efficient wet air oxidation and photocatalytic oxidation catalysts for the degradation of acetaminophen in aqueous phase. *Ecotoxicology and Environmental Safety*, *182*, 109367. https://doi.org/10.1016/j.ecoenv.2019.109367

Panplado, K., Subsadsana, M., Srijaranai, S., & Sansuk, S. (2019). Rapid Removal and Efficient Recovery of Tetracycline Antibiotics in Aqueous Solution Using Layered Double Hydroxide Components in an In Situ-Adsorption Process. *Crystals*, *9*(7), 342. https://doi.org/10.3390/cryst9070342

Papa, E., & Gramatica, P. (2008). Screening of persistent organic pollutants by QSPR classification models: A

comparative study. *Journal of Molecular Graphics and Modelling*, *27*(1), 59–65. https://doi.org/10.1016/j.jmgm.2008.02.004

Ren, L., Wang, C., Li, W., Dong, R., Sun, H., Liu, N., & Geng, B. (2019). Heterostructural NiFe-LDH@Ni_3S_2 nanosheet arrays as an efficient electrocatalyst for overall water splitting. *Electrochimica Acta*, *318*, 42–50. https://doi.org/10.1016/j.electacta.2019.06.060

Reyes, C., Fernández, J., Freer, J., Mondaca, M. A., Zaror, C., Malato, S., & Mansilla, H. D. (2006). Degradation and inactivation of tetracycline by TiO_2 photocatalysis. *Journal of Photochemistry and Photobiology A: Chemistry*, *184*(1–2), 141–146. https://doi.org/10.1016/j.jphotochem.2006.04.007

Rokesh, K., Sakar, M., & Do, T.-O. (2021). Emerging Hybrid Nanocomposite Photocatalysts for the Degradation of Antibiotics: Insights into Their Designs and Mechanisms. *Nanomaterials*, *11*(3), 572. https://doi.org/10.3390/nano11030572

Rosmini, C., Tsoncheva, T., Kovatcheva, D., Velinov, N., Kolev, H., Karashanova, D., … Lázaro, M. J. (2022). Mesoporous Ce–Fe–Ni nanocomposites encapsulated in carbon-nanofibers: Synthesis, characterization and catalytic behavior in oxygen evolution reaction. *Carbon*, *196*(April), 186–202. https://doi.org/10.1016/j.carbon.2022.04.036

Rouquerol, F., Rouquerol, J., Sing, K. S. W., Maurin, G., & Llewellyn, P. (2014). Introduction. In *Adsorption by Powders and Porous Solids: Principles, Methodology and Applications: Second Edition* (pp. 1–24). Elsevier. https://doi.org/10.1016/B978-0-08-097035-6.00001-2

Sahoo, D. P., Patnaik, S., & Parida, K. (2019). Construction of a Z-Scheme Dictated WO_{3-X}/Ag/ZnCr LDH Synergistically Visible Light-Induced Photocatalyst towards Tetracycline Degradation and H_2 Evolution. *ACS Omega*, *4*(12), 14721–14741. https://doi.org/10.1021/acsomega.9b01146

Samanidou, V. F., Nikolaidou, K. I., & Papadoyannis, I. N. (2007). Advances in chromatographic analysis of tetracyclines in foodstuffs of animal origin - A review. *Separation and Purification Reviews*, *36*(1), 1–69. https://doi.org/10.1080/15422110600822758

Sarmah, A. K., Meyer, M. T., & Boxall, A. B. A. (2006). A global perspective on the use, sales, exposure pathways, occurrence, fate and effects of veterinary antibiotics (VAs) in the environment. *Chemosphere*, *65*(5), 725–759. https://doi.org/10.1016/j.chemosphere.2006.03.026

Shi, W., Ren, H., Li, M., Shu, K., Xu, Y., Yan, C., & Tang, Y. (2020). Tetracycline removal from aqueous solution by visible-light-driven photocatalytic degradation with low cost red mud wastes. *Chemical Engineering Journal*, *382*, 122876. https://doi.org/10.1016/j.cej.2019.122876

Shi, Z., Wang, Y., Sun, S., Zhang, C., & Wang, H. (2020). Removal of methylene blue from aqueous solution using Mg-Fe, Zn-Fe, Mn-Fe layered double hydroxide. *Water Science and Technology*, *81*(12), 2522–2532. https://doi.org/10.2166/wst.2020.313

Sirisomboonchai, S., Li, S., Yoshida, A., Li, X., Samart, C., Abudula, A., & Guan, G. (2019). Fabrication of NiO Microflake@NiFe-LDH Nanosheet Heterostructure Electrocatalysts for Oxygen Evolution Reaction. *ACS Sustainable Chemistry and Engineering*, *7*(2), 2327–2334. https://doi.org/10.1021/acssuschemeng.8b05088

Soltani, T., Tayyebi, A., & Lee, B. K. (2019). Photolysis and photocatalysis of tetracycline by sonochemically heterojunctioned $BiVO_4$/reduced graphene oxide under visible-light irradiation. *Journal of Environmental Management*, *232*(September 2017), 713–721. https://doi.org/10.1016/j.jenvman.2018.11.133

Song, C., Liu, Y., Wang, Y., Tang, S., Li, W., Li, Q., … Lei, Y. (2021). Highly efficient oxygen evolution and stable water splitting by coupling NiFe LDH with metal phosphides. *Science China Materials*, *64*(7), 1662–1670. https://doi.org/10.1007/s40843-020-1566-6

Song, Z., Gao, H., Liao, G., Zhang, W., & Wang, D. (2022). A novel slag-based Ce/TiO_2@LDH catalyst for visible light driven degradation of tetracycline: performance and mechanism. *Journal of Alloys and Compounds*, *901*, 163525. https://doi.org/10.1016/j.jallcom.2021.163525

Tagliazucca, V., Schlichte, K., Schüth, F., & Weidenthaler, C. (2013). Molybdenum-based catalysts for the decomposition of ammonia: In situ X-ray diffraction studies, microstructure, and catalytic properties. *Journal of Catalysis*, *305*, 277–289. https://doi.org/10.1016/j.jcat.2013.05.011

Thi, L. N., Phan, T. T. T., Ngoc, T. N., Viswanath, N. S. M., Le, H. T. T., Tran Thi, L., … Vo, V. (2022). Prussian

Blue decorated g-C_3N_4 – From novel synthesis to insight study on charge transfer strategy for improving visible-light driven photo-Fenton catalytic activity. *Journal of Alloys and Compounds*, *916*, 165331. https://doi.org/10.1016/j.jallcom.2022.165331

Utami, H. P., Ahmad, N., Zahara, Z. A., Lesbani, A., & Mohadi, R. (2022). Green Synthesis of Nickel Aluminum Layered Double Hydroxide using Chitosan as Template for Adsorption of Phenol. *Science and Technology Indonesia*, *7*(4), 530–535. https://doi.org/10.26554/sti.2022.7.4.530-535

Wei, L., Li, Z., Ye, G., Rietveld, L. C., & van Halem, D. (2022). Comparative study of low-cost fluoride removal by layered double hydroxides, geopolymers, softening pellets and struvite. *Environmental Technology (United Kingdom)*, *43*(27), 4306–4314. https://doi.org/10.1080/09593330.2021.1946600

Wu, S., Hu, H., Lin, Y., Zhang, J., & Hu, Y. H. (2020). Visible light photocatalytic degradation of tetracycline over TiO_2. *Chemical Engineering Journal*, *382*, 122842. https://doi.org/10.1016/j.cej.2019.122842

Yan, J., Chen, Y., Qian, L., Gao, W., Ouyang, D., & Chen, M. (2017). Heterogeneously catalyzed persulfate with a CuMgFe layered double hydroxide for the degradation of ethylbenzene. *Journal of Hazardous Materials*, *338*, 372–380. https://doi.org/10.1016/j.jhazmat.2017.05.007

Yang, L., Li, L., Liu, Z., Lai, C., Yang, X., Shi, X., … Tang, C. (2022). Degradation of tetracycline by FeNi-LDH/Ti_3C_2 photo-Fenton system in water: From performance to mechanism. *Chemosphere*, *294*(November 2021), 133736. https://doi.org/10.1016/j.chemosphere.2022.133736

Yildirim-Tirgil, N., Lee, J., Cho, H., Lee, H., Somu, S., Busnaina, A., & Gu, A. Z. (2019). A SWCNT based aptasensor system for antibiotic oxytetracycline detection in water samples. *Analytical Methods*, *11*(20), 2692–2699. https://doi.org/10.1039/c9ay00455f

Yuan, J., Zhou, H., Li, D., & Xu, F. (2023). Construction of Fe_3S_4/g-C_3N_4 composites as photo-Fenton-like catalysts to realize high-efficiency degradation of pollutants. *Ceramics International*. https://doi.org/10.1016/j.ceramint.2023.01.205

Zhou, H., Wang, S., Jiang, J., Shao, L., Li, D., Yuan, J., & Xu, F. (2022). Magnetic Fe_3S_4/MoS_2 with visible-light response as an efficient photo-Fenton-like catalyst: Validation in degrading tetracycline hydrochloride under mild pH conditions. *Journal of Alloys and Compounds*, *921*, 166023. https://doi.org/10.1016/j.jallcom.2022.166023

Zhu, Z., Yang, R., Zhu, C., Hu, C., & Liu, B. (2021). Novel Cu-Fe/LDH@$BiOI_{1.5}$ photocatalyst effectively degrades tetracycline under visible light irradiation. *Advanced Powder Technology*, *32*(7), 2311–2321. https://doi.org/10.1016/j.apt.2021.05.008